*Int. J. Electrochem. Sci.*, 13 **(2018)** 9771 – 9783, doi: 10.20964/2018.10.43

International Journal of
ELECTROCHEMICAL
SCIENCE
www.electrochemsci.org

# Effect of Temperature and Voltage on the Preparation of Solid Carbon by Electrolysis of a Molten $CaCO_3$-$Li_2CO_3$-LiCl Electrolyte

*Karen Wong Min Jin*[1], *Miron Gakim*[1], *Jidon A. Janaun*[2], *Willey Liew Y. H.*[1], *Nancy J. Siambun*[1,3,*]

[1] Mechanical Engineering Programme, Faculty of Engineering, Universiti Malaysia Sabah, Jalan UMS 88400 Kota Kinabalu, Sabah, Malaysia
[2] Chemical Engineering Programme, Faculty of Engineering, Universiti Malaysia Sabah, Jalan UMS 88400 Kota Kinabalu, Sabah, Malaysia
[3] Material and Mineral Research Unit, Faculty of Engineering, Universiti Malaysia Sabah, Jalan UMS 88400 Kota Kinabalu, Sabah, Malaysia
[*]E-mail: nancyjs@ums.edu.my

*Received:* 22 April 2018 / *Accepted:* 12 June 2018 / *Published:* 1 September 2018

The present study investigated the preparation of solid carbon through the electrolysis of a newly formulated molten salt electrolyte containing $CaCO_3$–$Li_2CO_3$–LiCl with a continuous cell voltage of 4 – 6V, and temperatures of 550 and 650°C. The process was carried out in a two-electrode cell using AISI 304 stainless steel electrodes in $CO_2$ gas environment. $CO_2$ gas was captured and electro-converted to solid carbon, and deposited on the cathode surface. SEM images revealed five dominant microstructures: grape-like, tubes, thread-like, spheres, and flakes. These materials consist of 69 – 80% carbon content based on EA analysis. Single wall nanotube structures of 13 – 90nm outer diameter was also detected under TEM analysis. The result revealed that electrolysis voltage and temperature changes affected the microstructures, quantity of the deposited carbon, and the efficiency of electro-conversion process. The size of the carbon microstructures declined, and carbon deposition rate increased as both voltage and temperature were increased. However, it reduced the efficiency of the process**,** thus using more energy per g of carbon produced.

**Keywords:** Carbon, electro-deposition, electrolysis, molten salts, effect, temperature, voltage.

## 1. INTRODUCTION

Electrochemical conversion of $CO_2$ gas into fuels or solid carbon has attracted the attention of many researchers, industries and governments due to its amenability to automation and the increasing interest towards renewable energy [1]. Therefore, the electro-conversion of $CO_2$ gas to solid carbon is

widely reported; mostly through a process using a molten salt electrolyte containing a carbonate [1–5], or mixture of carbonate and chloride [6–8] in which solid carbon was deposited on the cathode surface. Various mixtures have been reported, including pure carbonate salt mixtures of $Li_2CO_3$–$Na_2CO_3$–$K_2CO_3$ [1,4,9], $Li_2CO_3$–$K_2CO_3$ [3,10], $Na_2CO_3$–$K_2CO_3$ and $CaCO_3$–$Na_2CO_3$–$K_2CO_3$ [11], and carbonate-chloride salt mixtures of $K_2CO_3$–KCl–LiCl [12], $Li_2CO_3$–LiCl [7,13], $CaCO_3$–$CaCl_2$–LiCl–KCl [10], and $Na_2CO_3$–LiCl–NaCl [14]. Despite the successful deposition of carbon with one or more alkali or alkaline-earth metal carbonates in the presence of a molten salt [1,2,4,7,10,13,15], the selection of the salt mixture was not clearly explained by the researchers.

The vast selection of salts makes it challenging to identify the optimum salt mixture to use as a medium for the electro-conversion process, but most studies preferred to use an alkali carbonate. The presence of carbonate ions ($CO_3^{2-}$) has been shown to substantially increase the amount of carbon deposited [16]. The carbonate ions were directly reduced to carbon and oxide ions at the cathode. In turn, the oxide ions reacted with $CO_2$ to regenerate the carbonate ions given $CO_2$ gas was supplied throughout the electrolytic process [3,10]. In this research, the molten salt was formulated to have low electrochemical stability but with high ability to absorb and convert $CO_2$ to carbon. In addition, the melting temperature was lowered to reduce energy consumption.

Studies revealed that both electrolysis voltage and temperature have a direct effect on the characteristics of the carbon produced. Using pure carbonate salt, Tang *et al.* [1] and Yin *et al.* [2] claimed that in the electro-deposition from a $Li_2CO_3$–$Na_2CO_3$–$K_2CO_3$ mixture, the carbon particle size decreased as the voltage increased. Similar observations were reported by Ijijie *et al.* [3] when using $Li_2CO_3$–$K_2CO_3$ mixture. In studies on the effect of electro-deposition temperature in a $Li_2CO_3$–$Na_2CO_3$–$K_2CO_3$ mixture by Tang *et al.* [1] and Van *et al.*[4], it was found that carbon particle size increased when deposition temperature was increased. By contrast, Ijijie *et al.* [3] reported that particle size reduced as temperature was increased for carbon electro-deposition in a $Li_2CO_3$–$K_2CO_3$ mixture. Ge *et al* [14] studied the effect of voltage and temperature variation for a carbonate-chloride mixture of $Na_2CO_3$–LiCl–NaCl, and reported that the quasi-spherical particle shape changed as voltage increased. At high voltage and temperature, the current efficiency decreased due to formation of lithium carbide or alkali metals at high voltage. In addition, the accumulation of carbon debris at the bottom of the melt also affected the process performance. In this work, the effects of electrolysis temperature and voltage were examined in the newly formulated $CaCO_3$-$Li_2CO_3$-LiCl mixture to determine their impact on the carbon particle size, microstructures, current efficiency, and energy consumption for the process.

## 2. EXPERIMENTAL

### *2.1 Chemical and materials*

The newly formulated salt was prepared using as-received $CaCO_3$ (extra pure; Bendosen), $Li_2CO_3$ (extra pure; HmbG) and LiCl salts (extra pure; HmbG). The ternary mixture of $CaCO_3$-$Li_2CO_3$-LiCl (mole ratio 0.09:0.28:0.63) has a liquidus temperature between 490 – 500°C.

Composition selection is further discussed in the results and discussion section. The mixed salt was contained in a custom-made stainless steel conical crucible (wall thickness: 1mm; dimensions: 80mm top-OD × 50mm base-OD × 120mm height). Stainless steel rods (type AISI 304; Cr 18 wt. %, Si 0.75 wt. %, C 0.08 wt. %, Mn 2 wt. %, P 0.045 wt. %, S 0.03 wt. %, Ni 8 wt. %, N 0.10 wt. % and Fe 71 wt. % with diameter of 9 mm) were employed for both the anode and cathode.

*2.2 Carbon Electro-deposition*

The electro-deposition process was carried out in a two-electrode configuration in a sealed reactor made of stainless steel AISI 304 as shown in Fig. 1. $CO_2$ gas was continuously purged in at 200mL/min rate. The electrolytic process was initiated by applying a constant cell voltage using an Agilent E3633A 20A DC power supply. The process was carried out for 3 hours to accumulate a sufficient amount of carbon for the subsequent analyses.

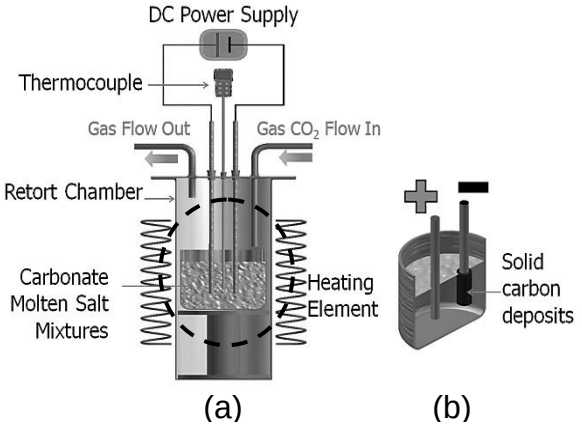


**Figure 1.** Schematic diagram (not according to scale) of (a) experimental set-up and (b) solid deposition on cathode surface for electro-deposition of solid carbon via electrolysis of ternary salt mixture, $CaCO_3$-$Li_2CO_3$-LiCl, in $CO_2$ gas environment.

The effect of cell voltage (4, 5, and 6V) and electrolysis temperature (550 and 650°C) on the newly formulated $CaCO_3$-$Li_2CO_3$-LiCl salt mixture were investigated in this research. The collected solid carbon was continuously washed with 1mol/L HCl followed by warm water (~50°C) to completely remove any salt residue before drying in a vacuum oven at 80°C for 24 hours. The mass of the collected carbon samples was recorded. It was recognized that very small amounts of carbon may be lost during the washing. The very fine carbon powder was either suspended on the surface of water and washed off, or formed a fine black layer on the surface of glass utensils.

The bulk elemental composition of the dried deposits was analyzed using an elemental analyzer (EA, Elementar Vario Micro Cube). The microstructure of the dried carbon samples was characterized using scanning electron microscopy (SEM, Hitachi S3400N with PC-SEM software). The SEM system included an integrated energy dispersive X-ray system (EDX, Bruker Quantax with Esprit 1.9

software) which was used to obtain the elemental composition of the attained microstructures. Higher resolution analysis and imaging of the carbon microstructures were carried out using transmission electron microscopy (TEM, TECNAI G2 Spirit BioTWIN). The structural analysis of the dried deposits was observed using X-ray Powder Diffraction (XRD) (PANalytical X'Pert Pro Multipurpose Diffractometer which powered by Philips PW3040/60 X-ray generator) and Raman Spectroscopy (Micro-Raman spectroscopy UniRAM-3500 equipped with Andor SOLIS software).

The carbon mass in the collected dried deposits, carbon deposition efficiency and amount of energy used to produce a 1 kg of carbon deposition was calculated according to equation (1), (2) and (3) respectively.

$$Carbon\ mass\ (g) = Mass\ of\ deposit\ (g)\ \times\ C\ purity\ from\ EA\ (data\ refer\ Table\ 2) \quad (1)$$

$$Current\ efficiency\ (\%) = \frac{Carbon\ mass\ (g)}{Calculated\ theoretical\ carbon\ deposited\ from\ I-t\ plot\ (g)} X100\% \quad (2)$$

$$Energy\ consumption\ (kWh/kg) = \frac{Voltage\ (V)\ \times Charge\ passed\ \times\ (1h/3600s)}{Carbon\ mass\ (kg)\ \times\ Current\ efficiency} \quad (3)$$

## 3. RESULT AND DISCUSSION

### *3.1 Formulating salt mixture*

The salt mixture used in this work was formulated to produce an electrolyte that has (i) low electrochemical stability to allow reduction of carbonate ions to carbon, (ii) a high affinity of the metal oxide to $CO_2$ to regenerate carbonate ions, thereby allowing indirect absorption of $CO_2$ gas, and (iii) a low melting temperature to reduce energy consumption.

Reaction (4) shows the decomposition of carbonate-based salt into oxides, solid carbon, and oxygen, whereas reaction (5) shows the regeneration of carbonate-based salt.

$$M_{2/x}CO_3\ (s) \rightleftharpoons M_{2/x}O\ (l) + C\ (s) + O_2\ (g) \quad (4)$$

$$M_{2/x}O + CO_2 \rightleftharpoons M_{2/x}CO_3 \quad (5)$$

Of the alkali and alkaline earth carbonates, $BeCO_3$ ($\Delta G°_{600°C}$ = 69.1 kcal), $MgCO_3$ ($\Delta G°_{600°C}$ = 82.7 kcal), $CaCO_3$ ($\Delta G°_{600°C}$ = 104.5 kcal), $SrCO_3$ ($\Delta G°_{600°C}$ = 116.7 kcal), and $Li_2CO_3$ ($\Delta G°_{600°C}$ = 115.9 kcal) have the lowest electrochemical stability to form carbon, metal oxide and oxygen gas, according to reaction (4), and were therefore pre-considered as potential salts for the mixture. However, $MgCO_3$ was rejected due to its low thermal stability *i.e.* $\Delta G°_{400°C}$ = –3.9 kcal, while $SrCO_3$ were avoided due to its high melting temperature and $BeCO_3$ due to toxicity.

When considering the work of Espen [17] which shows that oxides play an important role in capturing or absorbing $CO_2$ gas, it can be seen that $Li_2O$ ($\Delta G°_{600°C}$ = –21.3 kcal) and CaO ($\Delta G°_{600°C}$ = –10 kcal) demonstrate a strong affinity to $CO_2$ during the reformation to carbonates

according to reaction (5). This indicates that both are strong candidates for the salt mixture. All $\Delta G°$ values were derived from HSC Chemistry 6 software (Outotec).

Finally, the melting temperature of a eutectic mixture of $CaCO_3$-$Li_2CO_3$ (662°C *m.p*) can be further reduced with addition of their respective chloride. The initial consideration to add chloride to the mixture was either as additive to the carbonate salt, or to add a carbonate to the eutectic carbonate-chloride of the other metal. Table 1 shows the possible salt mixtures that were considered. Experiments were conducted to determine the melting point of various salt mixtures consisting of $CaCO_3$, $Li_2CO_3$, and LiCl salt mixtures with small additions of $CaCO_3$, $CaCl_2$, $Li_2CO_3$, and/or LiCl, as listed in Table 1. The findings confirmed that a eutectic $Li_2CO_3$-LiCl mixture with 0.1mol $CaCO_3$ as additive (overall salt mixture mole ratio $CaCO_3$:$Li_2CO_3$:LiCl = 0.09:0.28:0.63) has the lowest melting temperature (490 ~500°C *m.p*), and was therefore used in this work.

**Table 1**. Solidus and liquidus temperatures of various ternary and quaternary salt mixtures consisting of $CaCO_3$, $Li_2CO_3$, LiCl and $CaCl_2$.

| Eutectic salt mixture | Additive salt | Solidus (°C) | Liquidus (°C) |
|---|---|---|---|
| $CaCO_3$-$Li_2CO_3$ (662°C m.p) | + 0.1mol LiCl | 515 | 555 |
| $CaCO_3$-$Li_2CO_3$ (662°C m.p) | + 0.1mol $CaCl_2$ | 545 | 575 |
| $CaCO_3$-$Li_2CO_3$ (662°C m.p) | + 0.1mol LiCl + 0.1mol $CaCl_2$ | 455 | 545 |
| $CaCO_3$-$CaCl_2$ (635°C m.p) | + 0.1mol $Li_2CO_3$ | 635 | 745* |
| $Li_2CO_3$-LiCl (512°C m.p) | + 0.1mol $CaCO_3$ | 465 | 495 |

*The volume reduced drastically when fully melted, suggesting thermal decomposition.

*3.2 Carbon electro-deposition.*

The conversion process takes place at the interface between the electrode and the molten salt [5] once the voltage is applied to initiate the electrolysis process. The conversion of $CO_2$ gas to solid carbon through an electrochemical process is explained in detail by other author [10]. To summarise: the $CO_3^{2-}$ ion is reduced to solid carbon through electrolysis, either by a single step process [5,18,19] according to reaction (6), or a two-step process [20,21] according to reaction (7) and (8).

$$CO_3^{2-} + 4e^- \rightarrow C\ (s) + 3O^{2-} \quad (6)$$

$$CO_3^{2-} + 2e^- \rightarrow CO_2^{2-} + O^{2-} \text{ then } CO_2^{2-} + 2e^- \rightarrow C\ (s) + 2O^{2-} \quad (7\ \&\ 8)$$

$$O^{2-} + CO_2\ (g) \rightleftharpoons CO_3^{2-} \quad (9)$$

The $CO_2$ was absorbed into the molten carbonate salt through reaction (9) or $O^{2-}$ ions transported to, and discharged at the inert anode to produce the $O_2$ gas. The decomposition of LiCl and formation of $Cl_2$ gas due to too high over potential is made thermodynamically unfavorable due to the presence of large amounts of $CO_3^{2-}$ and $O_2$ [22].

In this work, solid carbon was prepared at two electrolysis temperatures: 550 and 650°C. The 550°C temperature was selected as 50°C higher than the melting temperature of salt to ensure a completely molten state but with minimal energy usage. In a study by Lorenz *et al.* [23] using $Li_2CO_3$–$Na_2CO_3$–$K_2CO_3$ it was shown that the lowest temperature at which CO gas was detected was 775°C with a potential of –1.8 V (against a Pt wire reference electrode). As such, the second

temperature for investigation was set to 650°C to avoid formation of CO gas.

The lowest cell voltage reported by other researchers for preparation of solid carbon in a pure carbonate mixture of $Li_2CO_3$–$Na_2CO_3$–$K_2CO_3$ and a carbonate-chloride mixture $Li_2CO_3$–LiCl was ~2.8V [2] and ~2.2V [7] respectively. In this work, the newly formulated $CaCO_3$–$Li_2CO_3$–LiCl salt had successfully deposited carbon using a voltage of 2.5V at 550 and 650°C, in which a thin layer of carbon deposited on cathode surface. However, the electrolysis was carried out with 4 – 6V to increase the rate of reaction (4). Fig. 2 shows an example of deposits formed on the cathode after 3 hours of electrolysis process in $CaCO_3$-$Li_2CO_3$-LiCl electrolyte at 550°C under voltage supply of 4V. All the other deposits exhibit similar trait.


**Figure 2**. The example of deposited solid on the cathode surface after 3 hours of electrolysis process in $CaCO_3$-$Li_2CO_3$-LiCl electrolyte at 550°C under voltage supply of 4V.

The surface morphology of the deposit was dense and gritty, with no presence of craters, which confirms that there were no or very few retained CO bubbles. This demonstrates that there was no substantial reduction of $CO_3^{2-}$ ions, or reduction of $CO_2$ and oxidation of $CO_3^{2-}$ as described in [10]. Elemental analyses confirmed that solid deposits prepared under electrolysis voltages of 4, 5 and 6V and temperatures of 550 and 650°C consisted of 69 – 80% carbon (Table 2). At 550°C, increasing voltage resulted in slightly increased carbon purity (4 – 5% increase per V) due to the increased rate of reaction (4). The carbon prepared at 650°C was of generally higher purity at all voltages as compared to 550°C but showed no clear correlation with cell voltage.

**Table 2.** Elemental analysis of collected solid deposits prepared at 550 and 650°C with voltage supply of 4 – 6V.

| Sample | Temperature (°C) | Voltage (V) | C (%) | N (%) | H (%) | S (%) |
|---|---|---|---|---|---|---|
| C1 | 550 | 4 | 69.6 | 0.02 | 1.5 | 0.3 |
| C2 | | 5 | 74.6 | 0.04 | 1.3 | 0.2 |
| C3 | | 6 | 79.5 | 0.07 | 1.4 | 0.3 |
| C4 | 650 | 4 | 78 | 0.06 | 1.1 | 0.2 |
| C5 | | 5 | 74.6 | 0.05 | 0.9 | 0.2 |
| C6 | | 6 | 79.4 | 0.09 | 1 | 1.9 |

*3.3 Characterization of deposited carbon*

*3.3.1. Microstructure analysis.*

SEM images revealed that solid carbon prepared through electrolysis in the newly formulated salt mixture at 550 – 650°C and 4 – 6V cell voltage showed five dominant microstructures: grape-like, tubes, thread-like, spheres, and flakes, as shown in Fig. 3a – e respectively.

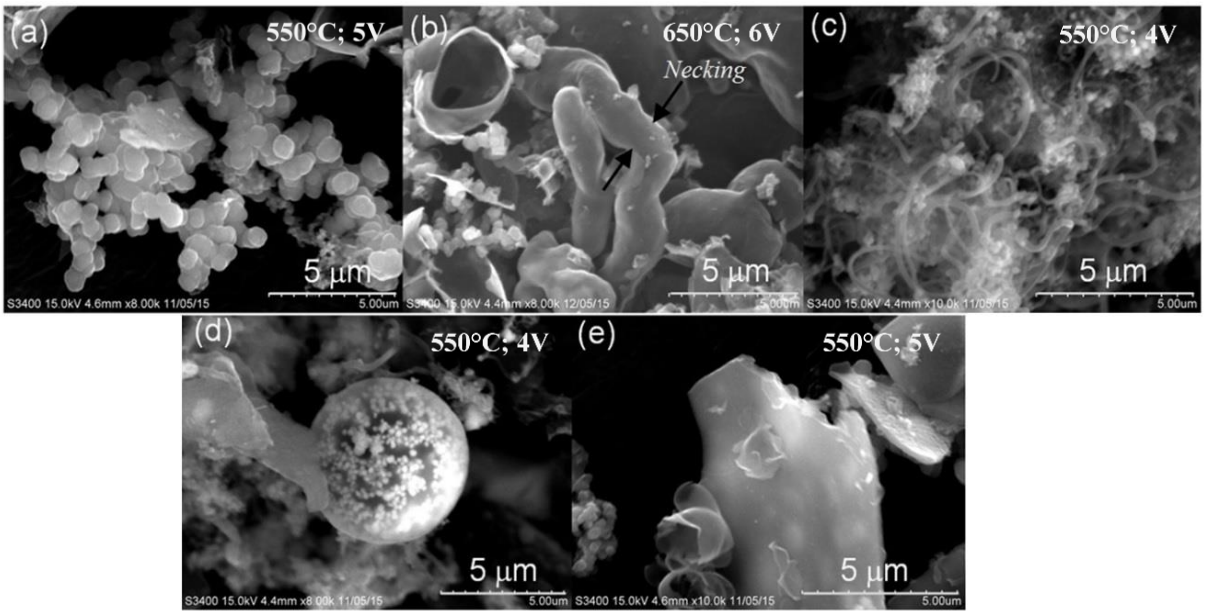


**Figure 3.** Example of SEM images for dominant microstructures found in the deposited samples prepared at 550 and 650°C with voltage supply of 4 – 6V, where (a) grape-like, (b) tubes, (c) thread-like, (d) sphere, and (e) flakes.

EDX elemental analysis shows that the all the microstructures have high carbon content *i.e.* >87 *at.* %, with tubes and flakes have >92 *at.*%. Traces of salt contaminants, due to inadequate washing and electrode, and crucible materials that corroded were also detected by EDX analysis.

The detected oxygen may be present as metal oxide in the salt residue or iron oxide, whereas the Au was from the gold-coating used for SEM analysis. The overall EDX elemental *at.* % for the various microstructures are listed in Table 3.

**Table 3**. The EDX elemental *at.* % for various carbon microstructure found in solid carbon prepared under 550 and 650°C with voltage supply of 4 – 6V.

| | | *Salt /post-prep.* | | *Electrode materials* | | | | *Others* | |
|---|---|---|---|---|---|---|---|---|---|
| Elements in *at.* % | C | Ca | Cl | Cr | Fe | Ni | S | O | Au |
| *Grape-like* | 87.7 | | 0.8 | | 0.2 | 0.01 | 0.02 | 11.3 | 0.05 |
| *Tubes* | 92.1 | 0.05 | 0.7 | 0.01 | 0.04 | | 0.02 | 7 | 0.06 |
| *Flakes* | 92.9 | 0.01 | 0.7 | | 0.01 | | 0.02 | 6.3 | 0.06 |
| *Thread-like* | 92.6 | 0.06 | 0.9 | 0.04 | 0.6 | 0.04 | 0.06 | 5.7 | 0.03 |
| *Sphere* | 88.4 | | 0.1 | | 1.4 | | | 10 | 0.02 |

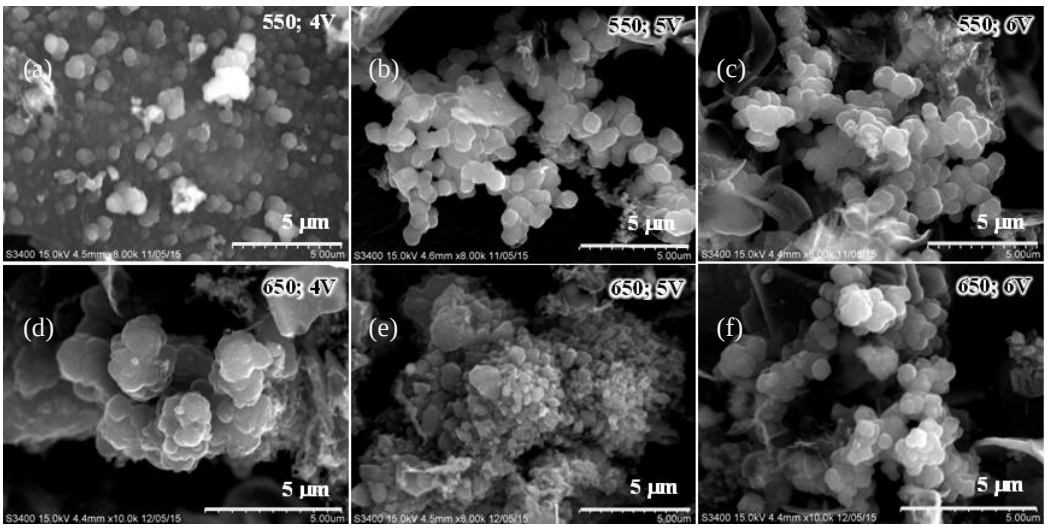


**Figure 4**. Agglomeration of grape-like microstructure with increasing voltage (a & d) 4V, (b & e) 5V and (c & f) 6V, and temperature (a – c) 550°C, (d – f) 650°C.

It is interesting to note that the carbon prepared at 550°C and 4V (the grape-like microstructure in Fig. 4a) became progressively agglomerated as cell voltage increased to 5V and 6V (Fig. 4b – c). At the same time, the diameter of the microstructure increased as indicated in Table 4. At the higher temperature of 650$^{o}$C the agglomeration was denser, diminishing the grape-like shapes, as shown in Fig. 4d – e. However, increasing the voltage to 6V seems to retain the grape-like shapes (Fig. 4f). The size however was smaller than that produced at 550$^{o}$C process. The sizes of these microstructures were listed in Table 4.

**Table 4.** Micro- and nano-structure shapes, and sizes of carbon samples obtained from SEM and TEM analysis.

| Temp. (°C) | Voltage (V) | Shapes and sizes of microstructure and nanostructure | | | | | | |
|---|---|---|---|---|---|---|---|---|
| | | Grape-like (µm) | Tubes (µm) | Thread-like (µm) | Sphere (µm) | Nanotubes *o.d* (nm) | Nanotubes *i.d* (nm) | Ring-like (nm) |
| 550 | 4 | 0.45–0.5 | 0.45–1.2 | 0.15–0.18 | 6.5–6.6 | 13–42.5 | 3–13.5 | 22–144 |
| 550 | 5 | 0.6–0.9 | 0.5–1.2 | - | 5.5–5.6 | 17–39.5 | 3–26 | 112–629 |
| 550 | 6 | 0.65–1.05 | 0.6–1.3 | - | 2.5–3 | 23.5–63 | 5–5.5 | 290–438 |
| 650 | 4 | *(a)* | - | 0.05–0.15 | - | 18–90 | 7–30 | 107–112 |
| 650 | 5 | *(a)* | - | - | - | 17–76 | 7–27.2 | 34–37 |
| 650 | 6 | 0.35–0.5 | 0.75–1.25 | - | - | 28–50 | 6–27 | 282–545 |

* *a*; agglomerates, *i.d*; internal diameter, *o.d*; outer diameter

The tubes microstructure seems to appear when the agglomerated grape-like microstructure as seen in Fig. 4b, 4c and 4f is present. Thus, it is proposed that the grape-like microstructure had built-up or elongated to become tubes as shown in Fig. 5. The SEM image in Fig. 3b also supports this mechanism because it shows that the tubes has necking instead of tubes with uniform diameter.

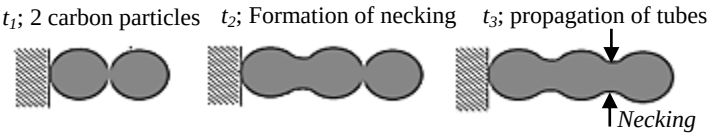


**Figure 5.** Linear progression of the particulates to single tube. *t* indicates time.

Thread-like (Fig. 3c) were produced under 4V cell voltage, and this microstructure is obtained at both 550 and 650°C. The diameter was found to reduce with increasing temperature as shown in Table 4. An interesting large spherical microstructure (Fig. 3d) was obtained when carbon was prepared at 550°C and 4 – 6V, with size decreasing with voltage increase. However, the spherical microstructure was not detected at 650°C. Flakes (Fig. 3e) seem to be a common microstructure and present abundantly at all temperature and voltage combinations.

TEM analysis revealed the presence of dispersed nanotubes microstructures (Fig. 6a) at all temperature and voltage combinations. The outer diameter of the CNTs varies from 13 to 97.5nm, while the internal diameter ranges from 3 to 30nm (Table 4). Under electrolysis at 550°C, the nanotubes size (outer diameter) increased as the voltage increased, whereas at 650°C the nanotubes size decreased as the voltage increased. Although preparation of carbon nanotubes via electrolysis is reported elsewhere [24–27], the process employed a chloride molten salt with a graphite cathode as the source of carbon. In the reported electrolysis process, the graphite cathode experienced erosion and electrolytically converted to carbon nanotubes in molten salt chlorides.

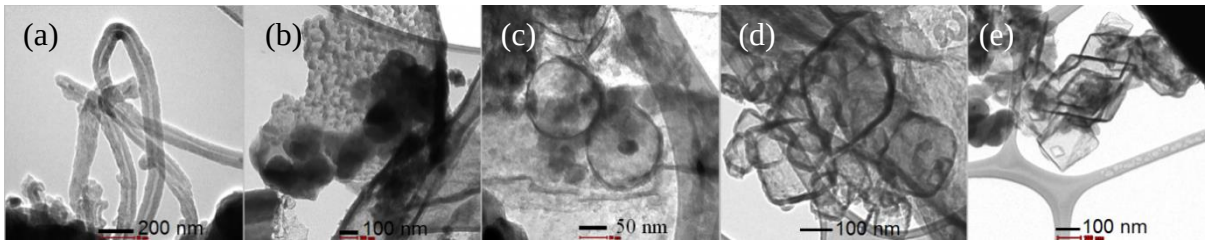


**Figure 6.** Example of TEM micrographs of (a) nanotubes, (b) amorphous, (c – e) ring microstructures on lacey support film, where the nano-structures were found in all deposited samples.

Agglomerate and ring-like amorphous microstructures were also detected in TEM analysis, similar to those reported by Kaplan *et al*. [19] and Ijije *et al*. [3]. Agglomerated amorphous carbon (Fig. 6b) and amorphous ring-like carbon with diameters between 22 – 629nm (Fig. 6c –e) were again found at all voltage and temperature combinations. The ring-like amorphous carbon appeared to be either circular (Fig. 6c) or square-shapes with either blunt (Fig. 6d) or sharp angles (Fig. 6e). Although Ijije *et al*. [3] reported that the ring-like microstructures of carbon deposited in $Li_2CO_3$–$K_2CO_3$ began to cleave as the voltage increased, this was not observed for carbon prepared in $CaCO_3$–$Li_2CO_3$–LiCl salt.

*3.3.2 XRD and Raman analyses*

The XRD patterns of the deposited carbon powders obtained at 550°C and 4 – 6V are displayed in Fig. 7. The two broad peaks that feature at $2\theta$ ~ 24° and 42° are typical of amorphous carbon [28]. This feature was observed in all carbon prepared at 550 – 650°C and 4 – 6V, which supports the results of the TEM analysis.

The broad (002) peak at $2\theta$ ~ 24° can be attributed to the graphitic carbon in the samples [29–31]. The broadness of the peaks indicates disordered carbon structures between the graphitic layers for all samples [28], and was again observed on all carbon prepared at 550°C and 4 – 6V. Although the intensity of this peak for carbon prepared at 5 and 6V and 550°C was comparable, the intensity was slightly higher for samples prepared at 4V. Increasing the electrolysis temperature to 650°C also decreased the intensity of the broad peak. The intensity changes suggest changes in the structure of the deposited carbon.

The peak at $2\theta$ ~ 42° was attributed to (100) diffraction of hexagonal graphite, and is supported by the work of Mohan and Manoj [31] who also claimed that the $2\theta$ ~ 42° peak is a signature of the hexagonal graphite lattice of multi-walled CNTs. However, it is also proposed by Ijije *et al*. [3] that this peak be attributed to magnetite $Li_5Fe_5O_8$.

Carbon prepared at 550°C and 4V exhibited the highest intensity peak at $2\theta$ ~ 42°. Carbon prepared at 5 and 6V are again comparable to each other but lower than that at 4V. Increasing the temperature slightly reduced the peak intensity for similar voltages. The intensity changes again suggest possible changes in the structure of the deposited carbon.

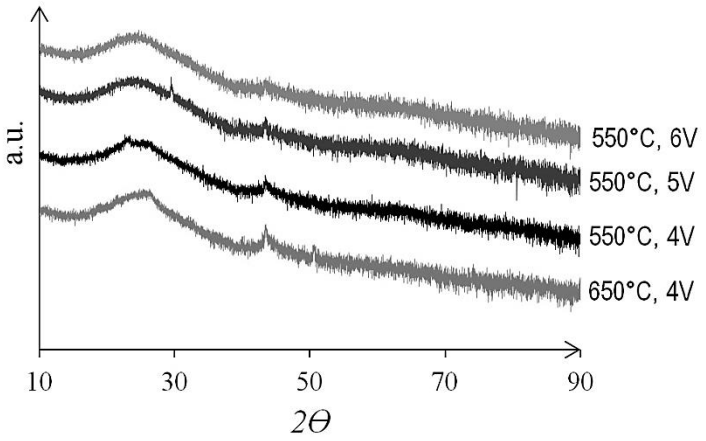


**Figure 7**. XRD pattern for deposited carbon prepared at 550°C under 4 – 6V and 650°C with 4V voltage supply.

The solid carbon samples were further characterized by Raman spectroscopy as shown in Fig. 8. The observation on Raman spectra is focused in the range 1000 – 2000 $cm^{-1}$. Within this range, peaks at 1600 and 1350 $cm^{-1}$ were visible for carbon prepared under all conditions. These peaks are characteristic of carbon material. The Raman peak at 1600 $cm^{-1}$ is attributed to crystalline graphite and usually called *G* band, whereas the peak at 1350 $cm^{-1}$ is referred to as *D* band and is due to structural disorder that breaks the translational symmetry *e.g.* impurities, edges, finite size effects, etc. [7,32].

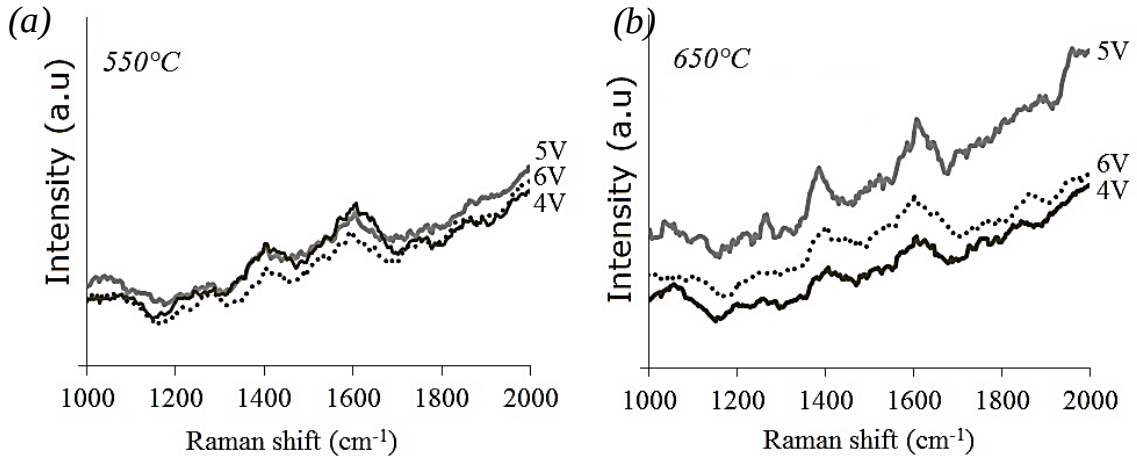


**Figure 8**. Raman spectra of carbon prepared at (a) 550 and (b) 650°C with voltage supply of 4 – 6V.

*3.4 Current efficiency and energy consumption*

The calculated carbon mass from the dried deposits according to equation (1) is listed in Table 5. As the voltage and temperature were increased, the mass of carbon increased, and this is due to the increased activity of $CO_3^{2-}$ under these conditions [3]. The efficiency of carbon deposition was calculated in terms of current efficiency using equation (2), while the amount of energy used to produce a 1kg carbon deposit at various temperatures and voltages was calculated with equation (3) [10]. The calculated values are listed in Table 5.

**Table 5.** Calculated values of carbon mass (g), current efficiency (%) and energy consumption (*kWh/kg*)

| Electrolysis temperature 550°C | | | | Electrolysis temperature 650°C | | | |
|---|---|---|---|---|---|---|---|
| Voltage (*V*) | Collected carbon mass (*g*) | Current Efficiency (%) | Energy consumption (*kWh/kg*) | Voltage (*V*) | Collected carbon mass (*g*) | Current Efficiency (%) | Energy consumption (*kWh/kg*) |
| 4 | 0.17 | 70.9 | 71.2 | 4 | 0.34 | 43.6 | 186.3 |
| 5 | 0.28 | 84.5 | 62.6 | 5 | 0.37 | *28.3 | 553.1 |
| 6 | 0.27 | 79.1 | 84.5 | 6 | 0.47 | 45.9 | 251.3 |

*value varies due to loss of very fine carbon particles during washing process.

For operation of the process at 550 and 650°C, the current efficiency ranges between 70 – 85% and 28 – 46%, respectively. The significant difference in these values indicates that process operation at 550°C is more efficient for carbon deposition. The decreased current efficiency at 650°C is due to the lower stability of the $CO_3^{2-}$ at higher temperature and this resulted in a shift in equilibrium towards the decomposition which reduced the absorption of $CO_2$. Moreover, the salt has greater electronic conductivity at increased temperature, meaning more current may be wasted just passing through the salt [33].

Further, these conditions resulted in the consumption of less energy to produce 1 kg of solid carbon. It is notable that energy consumption is not directly proportional to the value of the current efficiency. This is because energy consumption in electrolysis is predominantly dependent on the electrolyte temperature and electrochemical stability. The formation of $CO_3^{2-}$ and the subsequent formation of C could have different $\Delta G$s base on the temperature. The formation of carbon could either be a single step reaction (6) or two steps reactions (7 & 8). In the two steps reaction, charge is passed without the formation of carbon and would result in lowered current efficiency. Another factor that gives rise to an energy penalty is the required over potential in the electrode reactions and the electrolyte IR drop during the process [2].

The effect of voltage could not be clearly concluded, although for a fixed temperature, there were differences in current efficiency of up to 4% and 17% for 550 and 650°C, respectively.

## 4. CONCLUSION

Solid carbon was successfully deposited in a molten salt mixture of $CaCO_3$-$Li_2CO_3$-LiCl at 550 and 650°C and 4 – 6V applied cell voltage over a period of 3 hours. Carbon particles with various microstructures were produced, including grape-like, tubes, thread-like, spheres, and flakes. The effect of operating temperature and cell voltage on the microstructures and particles size was significant, and particles exhibiting sizes ranging from micro to nanometre scale were observed depending on the chosen parameters. TEM analysis revealed that deposited nanotubes outer diameter increased with increasing voltage at 550, and at 650°C the nanotubes size decreased. All carbon samples were amorphous carbon with a disordered structure. Increasing both process temperature and voltage lead to a change in carbon structure and degree of disorder. At high operating temperature and voltage, the rate of deposition was high due to the rapid nucleation of solid carbon. Current efficiency and energy consumption were more favorable for samples prepared at 550 compared to 650°C, where the optimum electro-deposition process at 550°C, 5V, attained current efficiency of 84.5% and energy consumption of 62.6 kWh/kg.

ACKNOWLEDGEMENT
The authors gratefully acknowledge support from Universiti Malaysia Sabah (UMS) and to Universiti Teknikal Malaysia (UTeM) Melaka for the analysis instrumentation.

*FUNDING*
This work was supported by Ministry of Science, Technology, and Innovation Malaysia (MOSTI) for the eScience Fund [MOSTI 06-01-10-SF0207].

## References

1. D. Tang, H. Yin, X. Mao, W. Xiao, and D.H. Wang. *Electrochim. Acta*, 114 (2013) 567.
2. H. Yin, X. Mao, D. Tang, W. Xiao, L. Xing, H. Zhu, D. Wang, and D.R. Sadoway, *Energ.*

*Environ. Sci.*, 6 (2013) 1538.
3. H. V. Ijije, C. Sun, and G.Z. Chen, *Carbon*, 73 (2014) 163.
4. K. Le Van, H. Groult, F. Lantelme, M. Dubois, D. Avignant, A. Tressaud, S. Komaba, N. Kumagai, and S. Sigrist, *Electrochim. Acta*, 54 (2009) 4566.
5. M.D. Ingram, B. Baron, and G.J. Janz, *Electrochim. Acta*, 11 (1966) 1629.
6. I.A. Novoselova, N.F. Oliinyk, S.V. Volkov, A.A. Konchits, I.B. Yanchuk, V.S. Yefanov, S.P. Kolesnik, and M.V. Karpets, *Physica E Low Dimens. Syst. Nanostruct.*, 40 (2008) 2231.
7. J. Ge, L. Hu, W. Wang, H. Jiao, and S. Jiao, *ChemElectroChem*, 2 (2015) 224.
8. A.T. Dimitrov, G.Z. Chen, I.A. Kinloch, and D.J. Fray, *Electrochim. Acta*, 48 (2002) 91.
9. H. Groult, B. Kaplan, F. Lantelme, S. Komaba, N. Kumagai, H. Yashiro, T. Nakajima, B. Simon, and A. Barhoun, *Solid State Ionics*, 177 (2006) 869.
10. M. Gakim, L.M. Khong, J. Janaun, W.L. Yun Hsien, and N.J. Siambun, *Adv. Mat. Res*., 1115 (2015) 361.
11. S. Licht, Stabilization of STEP electrolyses in lithium-free molten carbonates, 2 (2012) 2–5. https://arxiv.org/pdf/1209.3512.
12. H. Kawamura, and Y. Ito, *J. Appl. Electrochem*., 30 (2000) 571.
13. A.T. Dimitrov, The Electrolytic Deposition Of Carbon From Molten $Li_2CO_3$, Proceedings of 3rd BMC-2003-Ohrid, R. Macedonia (2003) 338–343. RN:35066187.
14. J. Ge, S. Wang, L. Hu, J. Zhu, and S. Jiao, *Carbon*, 98 (2016) 649.
15. H. V Ijije, R.C. Lawrence, N.J. Siambun, S.M. Jeong, D. Jewell, D. Hu, and G.Z. Chen, *Faraday Discuss*, 172 (2014) 105.
16. F. Lantelme, B. Kaplan, H. Groult, and D. Devilliers, *J. Mol. Liq.*, 83 (1999) 255.
17. O. Espen, U.S. Patent US8540954B2 (2013).
18. L. Massot, P. Chamelot, F. Bouyer, and P. Taxil, *Electrochim. Acta*, 47 (2002) 1949.
19. B. Kaplan, H. Groult, A. Barhoun, F. Lantelme, T. Nakajima, V. Gupta, S. Komaba, and N. Kumagai, *J. Electrochem. Soc*., 149 (2002) D72.
20. Y.Ito, and H.Kawamura, The Electrochem. Soc. Proceedings, Edited by R.J.Gale, C.Blomgren and H.Kojima, Vol. PV92-16 of The 8th Inter. Symp. Molten Salts, NJ, (1992), 574.
21. Y.K. Delimarskii, V.I. Shapoval, and V.F. Grishchenko, *Doklady Akademii Nauk SSSR*, 6 (1968) 1332.
22. N.J. Siambun, H. Mohamed, D. Hu, D. Jewell, Y.K. Beng, and G.Z. Chen, *J. Electrochem. Soc*., 158 (2011) H1117.
23. P.K. Lorenz, and G.J. Janz, *Electrochim. Acta*, 15 (1970) 1025.
24. J.. Bai, A.-L. Hamon, A. Marraud, B. Jouffrey, and V. Zymla, *Chem. Phys. Lett*., 365 (2002) 184.
25. C. Schwandt, A.T. Dimitrov, and D.J. Fray, *J. Electroanal. Chem*., 647 (2010) 150.
26. G.Z. Chen, X. Fan, A. Luget, M.S.. Shaffer, D.J. Fray, and A.H. Windle, *J. Electroanal. Chem*., 446 (1998) 1.
27. A.R. Kamali, and D.J. Fray, *Carbon*, 56 (2013) 121.
28. V. Asokan, P. Kosinski, T. Skodvin, and V. Myrseth, *Front. Mater. Sci*., 7 (2013) 302.
29. V. Suresh Babu, and M.S. Seehra, *Carbon*, 34 (1996) 1259.
30. V.S. Babu, L. Farinash, and M.S. Seehra, *J. Mater. Res*., 10 (1995) 1075.
31. A.N. Mohan, and B. Manoj, *Int. J. Electrochem. Sci*., 7 (2012) 9537.
32. A.C. Ferrari, and J. Robertson, *Philos. Trans. A. Math. Phys. Eng. Sci*., 362 (2004) 2477.
33. J.Y. Kim, Y.S. Choi, S.E. Bae, I. Yum, D.H. Kim, J.W. Yeon, and K. Song, *Asian J. Chem*., 25 (2013) 7028.